

CO4-1 Small Angle Neutron Scattering Measurements of Sodium Oleate by KUR-SANS System

K. Hara, Y. Uemoto, S. Yoshioka,
M. Sugiyama¹ and T. Fukunaga¹

*Research Institute of Environment for Sustainability,
Faculty of Engineering, Kyushu University
¹Research Reactor Institute, Kyoto University*

INTRODUCTION: Colloidal disperse systems show interesting characters by the interaction between two ingredients: solvent (water in case of hydrocolloids) and dispersoid. The authors have been studying their features, especially focusing on the hydrogels in which the solvent is water and the dispersoid is polymer network, and have found very interesting features. In addition to the hydrogel system, there is another typical colloidal system which is also close to the daily life: the surfactant-water system. Because it is well-known that some surfactant systems also show a kind of network structures, there can be found common structural features in spite of their clear material difference. Under these circumstances, the authors have measured SANS profile of a surfactant system of sodium oleate (Fig.1).

EXPERIMENTS: The 1 wt% of sodium oleate was dissolved in heavy water and the solution was sealed into a quartz cell, then they had been left intact for 24 hours at room temperature. Then the SANS profiles were observed during the course of heat treatments of the specimen at temperatures in the order of room temperature (as prepared), 36 °C and 5 °C. The SANS experiments were performed with a KUR-SANS spectrometer installed at Kyoto University Reactor, Kumatori, Osaka, Japan.

RESULTS AND DISCUSSIONS: The turbidity feature during the heat treatment is shown in Fig.2. At room temperature (as prepared, Fig.2a), the specimen was turbid and a sort of flocculated structure could be seen. Then, by heating the specimen up to 36 °C, there was considerable change: the specimen became almost transparent (Fig.2b). The specimen had remained transparent for 6 hours after stopping the heat treatment. Then after having cooled the specimen for 6 hours at 5 °C, the solution turned turbid again, however, the internal structure was finer than the initial one (Fig.2c). The SANS profiles of the respective stages are described in Fig. 3. From the SANS profiles, it can be estimate that there are fractal structures in the first and last stages with the fractal dimension of 1.96 and 2.49 while, in the intermediate stage, the system is composed of spheres with the gyration radius of 25 Å. Detailed investigations are in preparation.

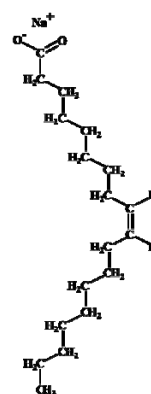


Fig.1. Structure of Sodium Oleate.

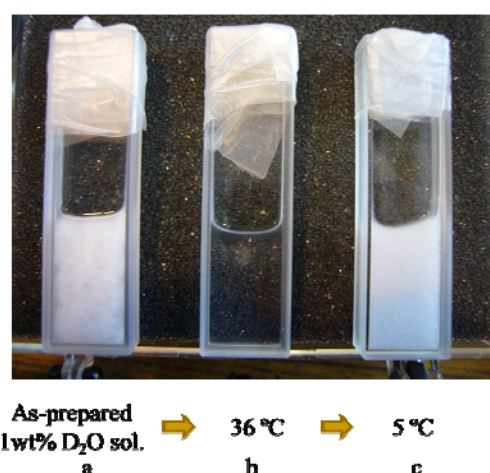


Fig.2. Turbidity Change by Heat Treatment.

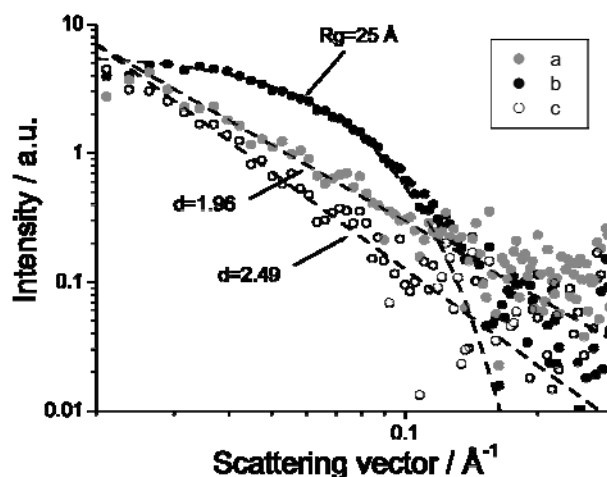


Fig.3. SANS Profile Change by Heat Treatment measured by KUR-SANS System. (see also Fig.2)

CO4-2 Radiation-Induced Luminescence for Applying to Retrospective Dosimetry

H. Fujita, Y. Nakano¹ and T. Saito¹

Nuclear Fuel Cycle Engineering Laboratories, JAEA
¹Research Reactor Institute, Kyoto University

INTRODUCTION: It is well known that natural quartz exposed to ionizing radiation emits both thermoluminescence (TL) such as violet TL (VTL), blue TL (BTL) and red TL (RTL), and optically stimulated luminescence (OSL) [1]. The luminescence phenomena have been used for retrospective dosimetry (e.g. [2, 3]). However, the reason for the emission mechanisms of their luminescences except for BTL [4] from Japanese quartz has not yet been well explained. In this study, the emission mechanisms of RTL, VTL and OSL were investigated in conjunction with radiation-induced phenomena after annealing treatments of quartz samples, involving TL OSL and electron spin resonance (ESR) measurements.

EXPERIMENTS: Coarse quartz grains (150~200 μm) collected from surface soils in Japan were extracted by a general treatment of 6M hydrochloric acid (HCl) and 6M sodium hydroxide (NaOH) followed by concentrated hydrofluoric acid (HF) and sieving treatments. Further purification of the quartz grains was performed by hand selection for the sake of elimination of feldspar grains as low as possible under a microscope. The extracted quartz samples were annealed using an electric furnace at numerous constant temperatures between 500 and 1000 $^{\circ}\text{C}$. After the annealing treatment, the quartz samples were irradiated with ^{60}Co source at room temperature at Kyoto University Research Reactor Institute (KURRI). After γ -ray irradiation (the applied dose: 1 kGy), the sample was stored at room temperature for one day to eliminate afterglow effect in dark room. The ESR measurement was carried out using an ESR spectrometer (Jeol Ltd., JES-TE 200) at room temperature and -196°C , respectively. The ESR signals were measured using the irradiated samples with blue-LEDs illumination or without the illumination. After the ESR measurements, all luminescence measurements were performed using a JREC automated TL/OSL-reader system installed with a small X-ray irradiator (Varian, VF-50J tube). All preparations were carried out under dim red light.

RESULTS: One kind of ESR signals was detected at room temperature (RT-centers). Furthermore, at -196°C the ESR signals of Ti-centers ($[\text{TiO}_4/\text{H}^+]^0$, $[\text{TiO}_4/\text{Li}^+]^0$ and $[\text{TiO}_4/\text{Na}^+]^0$) as the electron trapping center were measured together with Al-centers. These ESR signals were induced by γ -ray irradiation because they were not detected in quartz grains without the irradiation. Their intensities were changed with annealing temperatures. The amounts of $[\text{TiO}_4/\text{H}^+]^0$ centers gradually decreased with

annealing temperatures but the amounts of other Ti-centers, Al-centers and RT-centers increased with the temperatures. The comparison of ESR signals with blue-LED illumination and without one was carried out and then both signal intensities of the Al-centers and Ti-centers were decreased by the illumination. The other signal intensities were scattered.

The VTL and RTL glowcurves, and OSL decay curves were measured using all kinds of quartz samples. Their luminescence intensities increased with annealing temperatures as shown in **Fig. 1** and the shapes of their

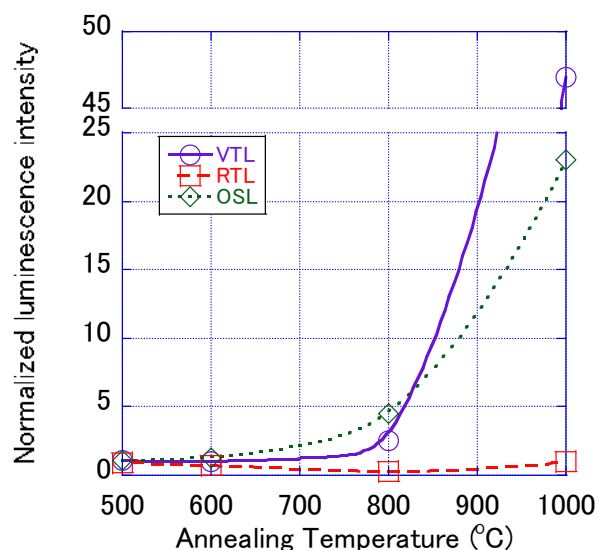


Fig. 1. Tendency of VTL, RTL and OSL intensities with several annealing temperatures. Each luminescence intensity was normalized to the intensity at 500 $^{\circ}\text{C}$.

curves were affected by annealing treatments. From the change of their curves, it was shown that trapping sites or electrons were affected by annealing treatments. Three kinds of luminescence intensities with blue-LED illumination were lower than the intensities without the illumination, respectively.

Further work is necessary to identify luminescence mechanism using ESR measurement and annealing experiment.

REFERENCES:

- [1] T. Yamaguchi *et al.*, BUNSEKI KAGAKU **52** (2003) 787-793.
- [2] T. Hashimoto *et al.*, Radioisotopes **51** (2002) 10-18.
- [3] T. Hashimoto *et al.*, Radiat. Meas. **41** (2006) 1015-1019.
- [4] T. Hashimoto *et al.*, BUNSEKI KAGAKU **51** (2002) 527-532.

S. Okuda, T. Kojima, D. Komatsu and T. Takahashi¹

Radiation Research Center, Osaka Prefecture University
¹Research Reactor Institute, Kyoto University

INTRODUCTION: The coherent synchrotron and transition radiation from electron bunches of a linac has continuous spectra in a submillimeter to millimeter wavelength range at extremely high peak-intensities. The coherent radiation (CR) light sources developed have been applied to absorption spectroscopy [1-4]. The light source can be used for matters with relatively strong light absorbance and for pulsed excitation of matters. Recently, the absorption spectroscopy system using the coherent transition radiation (CTR) from the electron beams of the 45 MeV L-band electron linac has been established at KURRI [5].

Microwave at submillimeter to millimeter wavelength range is used for heating in sintering powder materials. However, the processes for heating are not well known. In this work the absorption spectroscopy for the sample of SiO₂ fine particles has been performed by using the CR light source in order to investigate the light absorption process.

EXPERIMENTAL METHOD: The configurations for the absorption spectroscopy are schematically shown in Fig. 1. The output light from a Martin-Puplett type interferometer is focused at a light collimator 8 mmφ in diameter. The intensity of light is measured with a liquid-He-cooled silicon bolometer. The detailed method for the measurement is described in ref. 5.

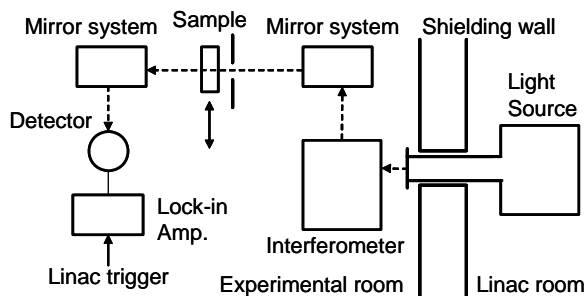


Fig. 1. Schematic diagram showing the configurations for absorption spectroscopy using the CR.

The sample of SiO₂ fine particles 5 mm thick has been sandwiched with two quartz plates 3 mm thick. The nominal averaged diameter of the particles is 26 nm.

The wavenumber resolution was 0.2 cm⁻¹ in the present experiments. It took about 5 minutes in a measurement. The light spectrum was obtained by averaging over four measurements. The spectrum was sufficiently stable during the measurements within ±2-3% in a wavenumber range of 4-12 cm⁻¹. The details of the light source are described in ref. 3.

In order to obtain the radiation at the lower intensity the electron injection current of the accelerator gun was decreased.

RESULTS AND DISCUSSION: The wavenumber dependence of the transmittance of light measured at relative light intensities of 1 and about 100 is shown in Fig. 2. Periodical oscillation observed in this figure corresponds to the interference of light in the sample. From the comparison with the results for the sample holder of two quartz plates it has been found that the sample has absorbed the light by 20-30% in this wavenumber range. The transmittance is higher by 20-30% at the higher intensity of light as shown in this figure. These results seem to suggest some change in the conditions of the sample induced by the pulsed CTR. The cause of this phenomenon will be investigated by changing the CTR conditions such as the intensity and the pulse length.

In order to investigate the transient phenomena induced by the pulsed CR pump-probe experimental system has been established in Osaka Prefecture University.

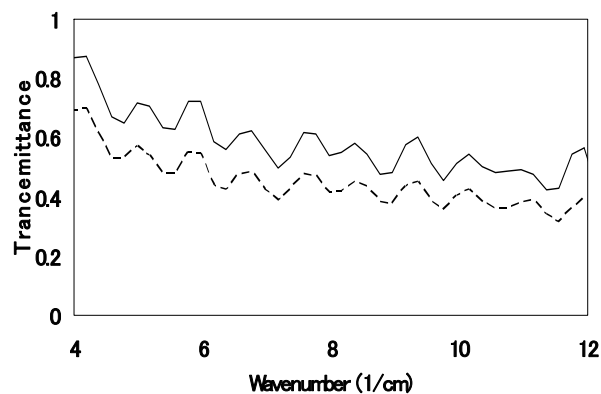


Fig. 2. Transmittance of CTR for the SiO₂ fine particle sample sandwiched with quartz plates 3 mm thick measured at relative light intensities of 1 (broken line) and 100 (solid line).

REFERENCES:

- [1] T. Takahashi, T. Matsuyama, K. Kobayashi, Y. Fujita, Y. Shibata, K. Ishi and M. Ikezawa, *Rev. Sci. Instrum.* **69** (1998) 3770.
- [2] K. Yokoyama, Y. Miyauchi, S. Okuda, R. Kato and T. Takahashi, *Proc. 20th Int. Free-Electron Laser Conf. (Williamsburg, USA, 2000) II* 17-18.
- [3] S. Okuda, M. Nakamura, K. Yokoyama, R. Kato and T. Takahashi, *Nucl. Instrum. Meth.* **A445** (2000) 267.
- [4] S. Okuda, M. Takanaka, M. Nakamura, R. Kato, T. Takahashi, S. Nam, R. Taniguchi and T. Kojima, *Radiat. Phys. Chem.* **75** (2006) 903.
- [5] S. Okuda and T. Takahashi, *Infrared Phys. Technol.* **51** (2008) 410.

Y. Okaue, T. Yokoyama and T. Sakudo

Department of Chemistry, Faculty of Sciences, Kyushu University

INTRODUCTION: Trimethylsilylated silsesquioxane, Q_8M_8 ($[(CH_3)_3SiO]_8(SiO_{1.5})_8$), is a member of the cage-shaped oligosilsesquioxanes with cubic framework called double four-ring (D4R) structure as illustrated in Fig. 1. Upon ^{60}Co γ -ray irradiation at room temperature on Q_8M_8 , stable hydrogen atom is encapsulated in D4R cage for the period of several years. The encapsulation and stabilization of hydrogen atom in D4R cage were confirmed by ESR spectroscopy. The hydrogen atom encapsulated in D4R cage of silsesquioxane interacts magnetically with paramagnetic oxygen molecules outside D4R cage to change ESR signal intensity and saturation behavior [1].

The purpose of this study was preliminary research for application of hydrogen atom encapsulated in D4R cage of silsesquioxanes such as development of oxygen molecule sensor. To encapsulate hydrogen atom in D4R cage of silsesquioxanes more efficiently, the effects of γ -ray irradiation conditions such as γ -ray dose, coexistence materials as the source of hydrogen atom, and side chain substituent groups of silsesquioxanes, were examined.

EXPERIMENTS: Silsesquioxanes with D4R cage structure used in this study were prepared by modifications of literature methods or obtained the commercially available compounds. Solid or viscous liquid samples were irradiated with γ -ray at total dose of 340-1700 kGy under air at room temperature in ^{60}Co γ -Ray Irradiation Facility at Kyoto University Research Reactor Institute. X-band ESR spectra for the irradiated samples under air, nitrogen, oxygen and vacuum were measured on a JEOL JES-FA200 spectrometer at room temperature.

RESULTS: Fig. 2 shows the typical ESR spectrum at room temperature of the hydrogen atom encapsulated in D4R cage of irradiated silsesquioxanes. Characteristic two hyperfine lines separated with about 50 mT due to hydrogen atom nucleus ($I=1/2$) were observed. ESR parameters (g value, A value, line width, saturation microwave power) were evaluated to investigate the states of hydrogen atoms encapsulated in D4R cage of various silsesquioxanes.

In this study, all measured g values for hydrogen atom encapsulated in D4R cage of irradiated silsesquioxanes were larger than 2.0023 of the g value for free hydrogen atom in vacuum. This result shows that electron of hydrogen atom obeys Pauli exclusion principle and $1s$ orbital of hydrogen atom interacts with $2p$ orbitals

of Si and O atoms of silsesquioxane cage. Shifts of g value for hydrogen atom in D4R cage of various silsesquioxanes were attributed to the degree of electron attraction of the side chain substituent groups. High electron attraction of the side chain substituent group enhances interactions between encapsulated hydrogen atom and atoms of silsesquioxane cage to give larger g value.

A value is hyperfine coupling constant that indicates strength of the interaction between nuclear spin and electron spin of hydrogen atom. This A value, which shows the contribution from Pauli exclusion force and dispersion force, increases by exclusion force and decreases by dispersion force. As the measured A values for hydrogen atom encapsulated in D4R cage of silsesquioxanes were smaller than 1420.4 MHz of the A value for free hydrogen atom in vacuum, dispersion force acts strongly and the strength depends on the electron attraction of Si atom of silsesquioxane cage to side chain substituent groups.

Line width, which defined the width between upper peak and lower peak of an ESR signal, increases with increasing oxygen concentration. This is because the paramagnetic oxygen molecules interact magnetically with hydrogen atom encapsulated in D4R cage of silsesquioxane to shorten the relaxation time. Saturation microwave power also increases with increasing oxygen concentration by shortening relaxation time of hydrogen atom in D4R cage of silsesquioxane and tends to increase as the length of side chain substituent group is long.

REFERENCE:

[1] R. Sasamori, Y. Okaue, T. Isobe, Y. Matsuda, *Science*, **265** (1994) 1691-1694.

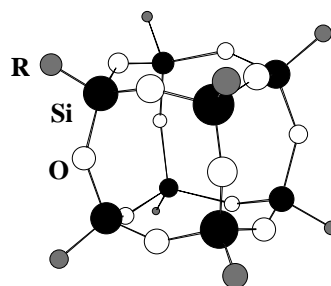


Fig. 1. D4R cage structure of silsesquioxane.
 $R = (CH_3)_3SiO$; Q_8M_8 .



Fig. 2. ESR spectrum of hydrogen atom encapsulated in D4R cage of irradiated Q_8M_8 .

CO4-5 The State Analysis of Gold on Magnetite Using ^{197}Au Mössbauer Spectroscopy

T. Yokoyama, Y. Okaue, Y. Katsuyama, T. Sakakibara, H. Ohashi¹ and Y. Kobayashi²

Faculty of Sciences, Kyushu University

¹Center for Research and Advancement in Higher Education, Kyushu University

²Research Reactor Institute, Kyoto University

INTRODUCTION: Gold supported on iron oxide is a good heterogeneous catalyst for mild oxidation of organic materials. However, as the support Fe_2O_3 has been used because of its stability and instability of Fe_3O_4 .

The aim of this study is to prepare $\text{Au}/\text{Fe}_3\text{O}_4$ catalysts using easy way and to characterize gold on these catalysts using ^{197}Au Mössbauer spectroscopy.

EXPERIMENTS: The catalysts were prepared by the general coprecipitation method. $\text{Fe}(\text{II})$ or $\text{Fe}(\text{III})$ aqueous solution with $\text{Au}(\text{III})$ was adjusted to proper pH and Eh. The chemical state of gold in the solid samples obtained was determined by ^{197}Au Mössbauer spectroscopy (home-made equipment). The ^{197}Pt isotope ($T_{1/2} = 18.3$ h), γ -ray source feeding the 77.3 keV Mössbauer transition of ^{197}Au , was prepared by neutron irradiation of isotopically enriched ^{196}Pt metal at the Kyoto University Reactor. The absorbers were particle specimens. The source and specimens were cooled with a helium refrigerator. The temperature of the specimens was in the range 8 – 15 K. The zero velocity point of the spectra was the peak point of pure bulk gold. The spectra for all the solid samples were fitted to a single Lorentzian function.

RESULTS: In a preliminary experiment, we found that magnetite can be synthesized easily by adjusting the $\text{Fe}(\text{II})$ solution to a suitable pH using oxidation of a part of $\text{Fe}(\text{II})$ to $\text{Fe}(\text{III})$ due to dissolved oxygen. In this reaction, if $\text{Au}(\text{III})$ is introduced, the $\text{Au}(\text{III})$ is reduced to $\text{Au}(\text{0})$ by $\text{Fe}(\text{II})$ under acidic condition. The $\text{Fe}(\text{II})$ solution including $\text{Au}(\text{III})$ was adjusted proper pH and Eh to cause stoichiometric deposition of magnetite supporting $\text{Au}(\text{0})$. According the powder X-ray analysis, the obtained solid sample was magnetite. Figure 1 shows ^{197}Au Mössbauer spectra for three solid samples including standards ((a) ferric hydroxide coprecipitating $\text{Au}(\text{III})$

before calcination, (b) after calcinations of the sample a as standards, and (c) magnetite coprecipitating $\text{Au}(\text{0})$ prepared in this study). As shown in Fig. 1, gold coprecipitated with hydrous ferric oxide was present as $\text{Au}(\text{III})$ before calcinations, but the $\text{Au}(\text{III})$ was thermally reduced to $\text{Au}(\text{0})$ after calcinations. On the other hand, even without calcination, gold supported on magnetite was present as $\text{Au}(\text{0})$ [1]. As a future work, we will measure a catalytic activity for the gold supported magnetite [2].

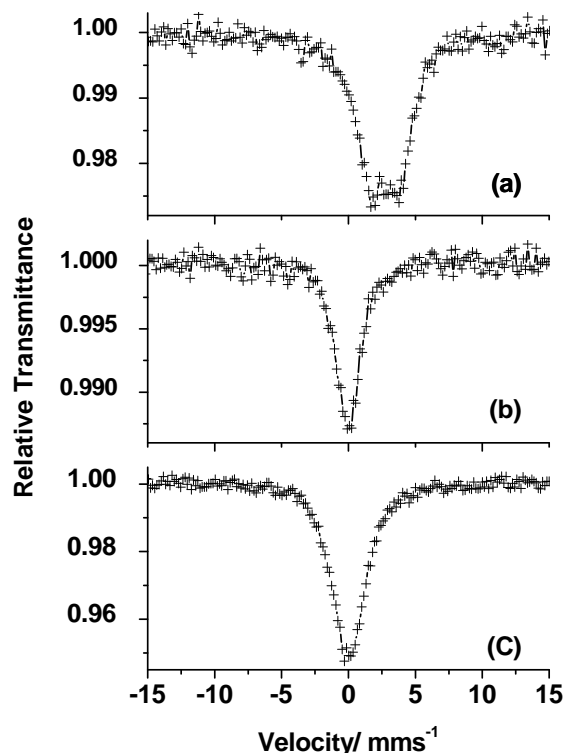


Fig. 1. ^{197}Au Mössbauer spectra for non-calcined (a) and calcined (b) $\text{Au}/\text{Fe}_2\text{O}_3$ prepared by CP method, and non-calcined $\text{Au}/\text{Fe}_3\text{O}_4$ (c).

REFERENCES:

- [1] T. Sakakibara, Master's Thesis, Kyushu Univ. (2011).
- [2] L.Liu *et al.*, *Dalton Trans.*, **19** (2008)2542-2548.

T. Awano and T. Takahashi¹

Department of Electronic Engineering, Tohoku Gakuin University

¹Research Reactor Institute, Kyoto University

INTRODUCTION: Movement of ions is not in phase and frequent scattering by other mobile ions seems to decrease the ionic conductivity. If coherent excitation of ionic movement by coherent external electric field occurs, ionic conductivity seems to increase drastically. We have investigated sub-millimeter and far-infrared spectroscopy of superionic conductors to find such a correlative movement of conduction ion. Ionic plasmon absorption was observed at sub-millimeter region of MA_4X_5 ($M=Rb, K, NH_4$; $A=Ag$ or Cu ; $X=I$ or Cl) crystals [1]. Coherent THz wave from LINAC of KURRI is so strong that the excitation effect is expected to be observed. We have measured millimeter wave absorption spectra of silver halides - silver phosphate glasses to investigate the existence of such a collective movement of conduction ion [2]. In this study, copper ion conductors were investigated to compare spectral deference by the mass of conduction ion.

EXPERIMENTS: Each content of CuI , Cu_2O and P_2O_5 were melt in Pyrex tube with N_2 atmosphere at 600 C for 30 min. Then the melt was quenched in water. Sample pellets with thicknesses around 1mm were obtained by pressing. Transmittance spectra of coherent millimeter wave were measured by a Martin-Puplett type interferometer.

RESULTS: Figure 1 shows absorption spectra of a $CuI-CuPO_3$ glasses. Increment spectra at 300K from absorption at 77K are shown to avoid interference fringe structure. Two absorption bands were observed as those in $AgI-AgPO_3$ glasses. Peak positions are, however, slightly different. They are 9.7 and 6.8 cm^{-1} for each temperature in the $CuI-CuPO_3$ glass, while they are 8.5 and 6.1 cm^{-1} $AgI-AgPO_3$ glasses. The peak positions of these bands are 15% and 10% larger than those in the $AgI-AgPO_3$ glasses. This seems to be due to difference of conduction ions, copper and silver. However, this ratio is smaller than that of the square root of the mass of conduction ion (1.3). This suggests that these bands are due to not only one mobile ion but also other ions. This is consistent with the result in bromides-silver phosphate glasses [3].

Figure 2 shows absorption spectra of a $AgI-Ag_2O-V_2O_5$ glass. Main feature of the spectra is the same as those of

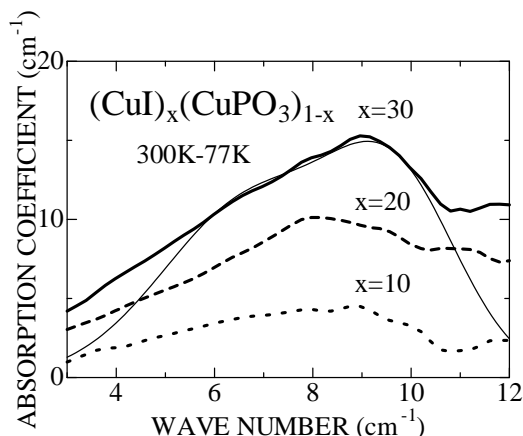


Fig. 1. Increment absorption spectra of $(CuI)_x(CuPO_3)_{1-x}$ glass at 300K from that at 77K. Thin line shows the summation of two Gaussian curves at 9.7 and 6.8 cm^{-1} .

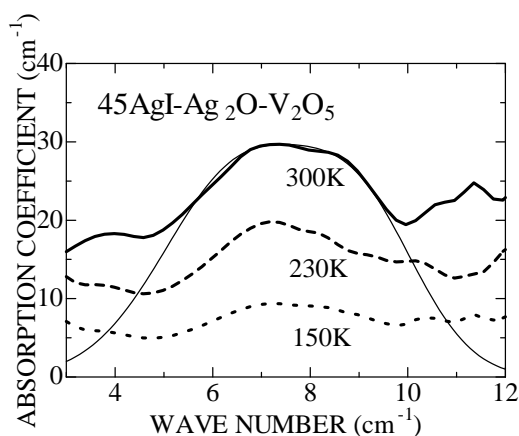


Fig. 2. Increment absorption spectra of $(AgI)_{0.45}(Ag_2O)_{0.33}(V_2O_5)_{0.22}$ glass from that at 77K. Thin line shows the summation of two Gaussian curves at 9.1 and 6.6 cm^{-1} .

$AgI-AgPO_3$ glasses. Peak positions of the two bands were slightly different from those in $AgI-AgPO_3$ glasses. This seems to be due to difference of glass network structure.

REFERENCES:

- [1] T. Awano, *Infrared Physics and Technology* **51**(2008) 458.
- [2] T. Awano and T. Takahashi, *Journal of Physics: Conference Series* **148** (2009) 012040.
- [3] T. Awano and T. Takahashi, *J. Phys. Soc. Jpn.* **79** Suppl. A (2010) 118.

T. Takahashi, T. Iizuka¹, T. Mori² and S. Kimura^{2,1}

Research Reactor Institute, Kyoto University

¹School of Physical Sciences, The Graduate University for Advanced Studies

²UVSOR Facility, Institute for Molecular Science

INTRODUCTION: The technique of near-field THz-wave microscopy is a characteristic application of coherent radiation emitted from a relativistic electron beam. This technique provides high spatial resolution below the diffraction limit. In the previous reports [1, 2] we obtained the spatial resolution power of $\lambda/4$ in the transmission and the reflection mode. In the calculation of the spatial resolution power we have used the wavelength at the peak intensity in the spectral distribution as the typical wavelength. However, it is important to investigate the dependence with wavelength experimentally for the wideband spectroscopy. In the present report we have been the dependence of spatial resolution with wavelength in the transmission mode using an aperture probe with coherent transition radiation (CTR).

EXPERIMENTAL PROCEDURES: The experiment was performed at the coherent radiation beamline [3] at the 40-MeV L-band linac of the Research Reactor Institute, Kyoto University. The width of the macro pulse and the repetition rate of the electron beam were 47 ns and 46 Hz, respectively. The charge of a bunch was 1.2 nC. The THz-wave source was CTR emitted from an aluminum foil with a thickness of 15- μm . The conical cone of Teflon coated by the silver paste on the tapered surface was used as an aperture probe. In order to investigate the spatial resolution, the edge of a stainless steel plate 0.3 mm thick was scanned as a sample in front of the aperture on the top of the illumination probe. The spectrum of CTR was measured by a Martin-Puplett type interferometer.

RESULTS: The spectra were obtained at each scanning position of the sample. Then the observed data were reconstructed to the scanning curves at each wavelength. The spatial resolution is equivalent to the width of the first derivative of the scanning curve. The calculated spatial resolutions were summarized in Table 1. The longer the wavelength became, the larger the resolution power became. The spectrum of the transmission wave was also shown by Fig. 1. It has two peaks at 5 and 10 cm^{-1} . The reason was

considered to be the interference inside the illumination probe of Teflon.

ACKNOWLEDGMENTS: This work was partly supported by Quantum Beam Technology Program of MEXT, Japan.

REFERENCES:

- [1] T. Takahashi, *et al.*, KURRI-PR 2008 (2009) CO4-10.
- [2] T. Takahashi, *et al.*, KURRI-PR 2009 (2010) CO4-8.
- [3] T. Takahashi, *et al.*, Rev. Sci. Instrum. **69** (1998) 3770.

Table 1. Dependence of spatial resolution power with wavelength

Wavenumber ν (cm^{-1})	Wavelength λ (μm)	Spatial Resolution Δx (μm)	Spatial resolution power $\lambda/\Delta x$
3.70	2700	371	7.3
4.94	2025	360	5.6
6.17	1620	341	4.8
7.41	1350	292	4.6
8.64	1157	243	4.8
9.88	1012	226	4.5
11.1	900.1	214	4.2
12.4	809.7	204	4.0
13.6	736.4	195	3.8
14.8	675.2	195	3.5
16.1	623.1	192	3.2
17.3	578.7	183	3.2

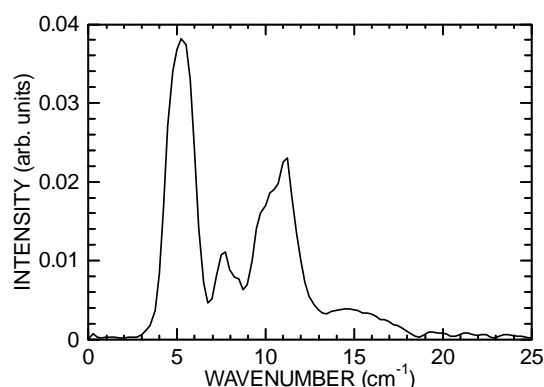


Fig.1. Observed spectrum of transmitted THz wave.

T. Takahashi

Research Reactor Institute, Kyoto University

INTRODUCTION: In recent years the THz-TDS has been widely used in the THz spectroscopy. The merit of the system is direct observation of the electric field. The spectroscopic system using a bolometer can detect only the power of THz wave. Therefore the Kramers-Kronig analysis is necessary in order to calculate the optical constant. One of the detection system in the THz-TDS is the Electro-Optical (EO) sampling in which the induced birefringence by the Pockels effect is used. In this report the EO sampling has been applied to the detection of coherent transition radiation (CTR). Usually an ultrafast laser is used as a probe light in the THz-TDS. The strong point in this report is the usage of Cherenkov radiation in the visible region as a probe light. There is no jitter between CTR and Cherenkov radiation.

EXPERIMENTAL PROCEDURES: The experiment was performed at the coherent radiation beamline [1] at the 40-MeV L-band linac of the Research Reactor Institute, Kyoto University. The width of the macro pulse and the repetition rate of the electron beam were 47 ns and 46 Hz, respectively. The average current of the electron beam was 1.8 μ A. The sub-THz radiation was the superposition of the forward CTR from the Ti-window and backward CTR from an aluminum-coated silica grass as shown in the Fig.1. The visible light for a probe of the EO-sampling was the Cherenkov radiation from a silica grass 5 mm thick. A ZnTe plate 1 mm thick was used as the EO device. The visible light was passed through a ZnTe plate, polarizer, a $\lambda/4$ retarder, and a Wollaston prism as shown in Fig.2. It was finally detected by a balanced detector which consists of two photo-diode detectors and amplified by a lock-in amplifier.

RESULTS: In order to investigate the Pockels effect an ITO grass plate was put in and out on the optical path as shown in Fig.2. The ITO grass has property that it reflects the THz wave and transmits the visible light. The THz wave was irradiated to ZnTe plate without the ITO grass plate. The result is shown in Fig.3. The average intensity

was 4.37 μ V with ITO grass and 5.04 μ V without it. Though the observed intensity was very small, the Pockels effect was able to be confirmed.

REFERENCES:

- [1] T. Takahashi *et al.*, Rev. Sci. Instrum. **69** (1998) 3770.

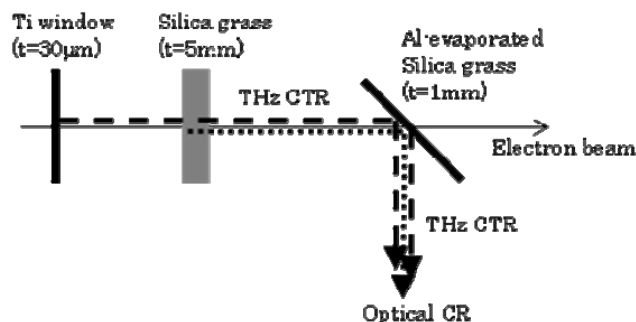


Fig.1. The schematic layout around the radiation source.

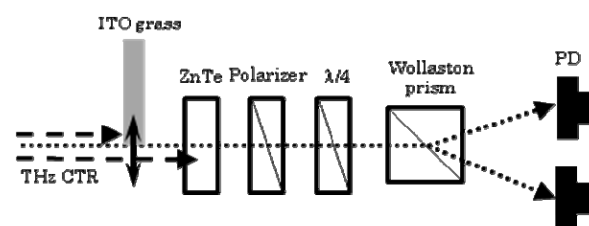


Fig.2. The schematic layout of the EO sampling.

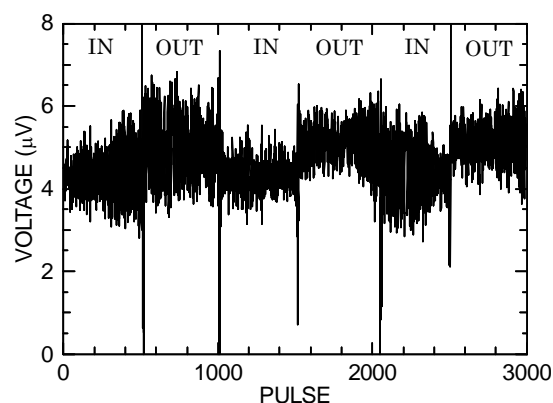


Fig.3. The observe intensity by the balance detector with and without the ITO grass, i.e., the THz-wave irradiation.

CO4-9 Complex Structure of Ions Coordinated with Hydrophilic Polymer. 11:

A. Kawaguchi, Y. Gotoh¹ and Y. Morimoto

Research Rector Institute, Kyoto University

¹Faculty of Text. Sci. and Tech., Shinshu Univ.

INTRODUCTION: We have reported *in situ* composite structure through "secondary doping" by diffusion of metallic ions into the iodinated hydrophilic polymers. Polyiodide ions, I_n^- ($n = 3, 5, \dots$), which have been doped into the polymers previously, enhances following diffusion of other molecules or ions even through solution process at room temperature [1,2]. In a case of silver cation, Ag^+ , its diffusion (secondary doping) into the iodinated polymers introduced complicated structures of composite and various stages on precipitation of inorganic fillers which showed both analogy and singularity to results given by environment within aqueous solution. For example, we provisionally suggested "stage I / II / III" of (hybrid) composite where diffusion of Ag^+ ion into matrix by hydrophilic polymers did not conclusively introduce unique structure or precipitation, while ionic reaction in aqueous solution generally produces precipitation of silver iodide, AgI [3]. One of these stages in composite, "stage III", which was prepared through excessive Ag^+ doping, often indicates white or colorless appearance even though inorganic elements have been maintained as dopants [4]. It may sound contradictory, but mass estimation suggested excessive doping of Ag^+ ion might induce decrease in precipitated inorganic filler [5]. And this "stage III" is relatively elastic and it shows opaque transparency while "stage I" is not transparent stage or "stage II" is stiff. Therefore, "stage III" or relevant procedures can be expected for application as optical devices or material processing.

EXPERIMENTS: Commercial products "Rayfan #1401" in thickness of 0.1mm which was presented by Toray Film co.ltd., was used as non-doped PA6 (polyamide-6, NylonTM-6). A strip cut from a PA6 sheet were stretched (x3-4) and was annealed at 210°C in vacuum. This strip was doped with I_2 -KI(aq) (0.2N) at 5°C for more than 5days and this process (iodine-doping) was terminated by rinsing with water. After drying in vacuum at R.T.(25°C) for 3 weeks, the sample was immersed in $AgNO_3$ (aq) (2M) at R.T. for more than 24hrs.

Optical observation was achieved by a CCD camera for translucency with a polarized beam incident generated by a He-Ne laser source; a polarizer was set in upper side of the sample. Stretching direction of the sample were set parallel or normal to polarization of the incident, and an analyzer was rotated for an angle of 0° (parallel to the polarizer) to 90° (normal to the polarizer).

RESULTS AND DISCUSSION: Samples which were excessively treated with $AgNO_3$ (aq) for secondary doping indicate white or colorless appearance though they keep inorganic components in their inner volume, and they are

modified softer than other stages (in some cases, softer than non-doped original matrix). We called such a stage "stage III" because analogous trend was observed for other matrixes of hydrophilic polymers, for (poly)vinyl-alcohol (PVA) or reproduced cellulose. On the other hand, "stage I" or "stage II" is stiffer than the iodinated matrix. Or, optical transparency of visible light through the "stage I", which is a stage introduced by moderate dealing with $AgNO_3$ (aq), is so low and it looks black or dark color as iodine [4].

Then, containment of inorganic fillers in oriented and transparent (often opaque) matrix let us expect optical anisotropy for polarization with transparent light, consequently. As results, anisotropy on polarization was confirmed for the polarized laser incident; transparent intensity through the oriented samples given by its drawn direction normal to incident polarity was relatively intense than data by the direction parallel to incident polarity (figure). It is qualitatively analogous to iodine-doped PVA which is applied as polarizer for wide-used optical devices like as displays for PC [6].

Results suggest that some components or structures exist as origin for polarization. However, it is not concluded yet if they are low molecular components (as metallic salts or some components attributed to polyiodides) or macromolecular structures. At least, it is regarded that ordinary iodine or polyiodide ions (I_3^-) do not exist similar as ordinarily shaped molecules with large absorption for visible light.

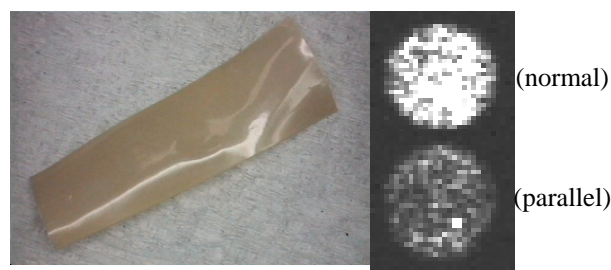


Fig.1. Optical anisotropy introduced within stretched PA6 film in "stage III"; stretching direction was normal to polarizer (upper) or parallel to it (lower). (Indicated pictures were observed in layout of 30° which is angle between polarizer and analyzer.)

REFERENCES:

- [1] A. Kawaguchi, *Sens. Actuators B*, **73** (2001) 174-178.
- [2] Y. Gotoh, *et.al.*, *Polym. Prep. Jpn.*, **51** (2002) 2259-2259.
- [3] A. Kawaguchi, *et.al.*, *ibid.*, **55** (2006) 1004-1004.
- [4] A. Kawaguchi, *et.al.*, *ibid.*, **56** (2007) 768-768.
- [5] Y. Gotoh, *et.al.*, (private communication)
- [6] Y. Oishi, *et.al.*, *Polym. J.*, **19** (1987) 331-336.

K. Okuno, Y. Oya, R. Kurata, M. Kobayashi, J. Osuo, M. Suzuki, A. Hamada, K. Matsuoka, K. Kawasaki, T. Fujishima, Y. Miyahara, T. Fujii¹, and H. Yamana¹

*Radioscience Research Laboratory, Faculty of Science,
Shizuoka University*

¹*Research Reactor Institute, Kyoto University*

INTRODUCTION: Many studies have been carried out to establish a tritium recovery system in fusion reactors. Especially, many researchers focus on lithium titanate (Li_2TiO_3) because it is one of the candidates as the tritium breeding material for ITER due to its good tritium recovery efficiency and chemical stability. It is necessary to clarify tritium behavior from the viewpoint of fuel cycle in neutron-irradiated Li_2TiO_3 . In our previous studies[1], tritium release behavior has a large correlation with the annihilation of irradiation defects, E'-center and oxygen hole centers, in neutron-irradiated Li_2TiO_3 , which were annealed by the recombination process in the temperature range of 500-650 K and whose activation energy was estimated to be 0.68 eV from the results of gamma-ray irradiation experiments for Li_2TiO_3 [2]. On the other hand, actual tritium trapping site and tritium release process have not been clarified in detail for neutron-irradiated Li_2TiO_3 .

In this study, thermal neutron irradiation was performed in order to elucidate actual tritium release behavior in Li_2TiO_3 . Thermal Desorption Spectroscopy (TDS) measurement with various heating rate and isothermal heating experiment were performed to understand tritium trapping site and tritium release behavior kinetically.

EXPERIMENTS: Li_2TiO_3 powder purchased from KAKEN Co., Ltd. was irradiated by thermal neutron with the fluence of $3.3 \times 10^{14-16} \text{ n cm}^{-2}$ at the Kyoto University Research Reactor Institute (KURRI). After neutron irradiation, the tritium release behavior was measured by TDS using proportional counters and total amount of released tritium was determined by a liquid scintillation counter. TDS measurement was performed with the heating rate of 5-30 K min^{-1} in the temperature range of 300-1373 K with D_2/He gas as purge gas. Isothermal heating measurement was also performed at some constant temperatures in temperature region of 548-773 K.

RESULTS: Figure 1 shows the Tritium TDS spectrum with a heating rate of 5 K min^{-1} for Li_2TiO_3 irradiated by

thermal neutron up to the fluence of $3.3 \times 10^{16} \text{ n cm}^{-2}$. It was found that about 95% of tritium was released as DTO form and the TDS spectrum has two desorption stages around 680 K (Peak 1) and 850 K (Peak 2).

Isothermal heating measurement showed that the rate-determining step of tritium release as Peak 1 was tritium detrapping from trapping site, whose activation energy was estimated to 0.65 eV, corresponding to that of recombination of E'-center and oxygen hole centers, indicating that trapping sites of tritium released as Peak 1 was irradiation defects and the rate-determining step of tritium release as Peak 1 was recombination of irradiation defects.

The Peak 2 was attributed to the desorption of tritium trapped as O-T bonds[3]. The activation energies for tritium release as Peak 2 have changed by the neutron fluence between 3.3×10^{14} , 3.3×10^{15} and $3.3 \times 10^{16} \text{ n cm}^{-2}$, which were calculated to be 0.48, 0.75 and 1.00 eV respectively, indicating that the rate-determining step of tritium desorption from O-T bond was decomposition of O-T bond via diffusion process of tritium through oxygen, which would have two types diffusion with different activation energies[4]. One diffusion process is that tritium diffuses by replacement with nearby lithium as bind to oxygen. The other process is that O-T bond is decomposed and tritium is re-trapped by another nearby oxygen. It was suggested that apparent activation energy was changed by ratio of each diffusion process and the amount of tritium influenced the ratio of each diffusion process.

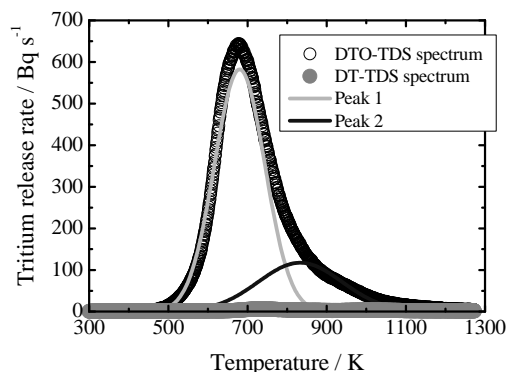


Fig.1. T-TDS spectrum for Li_2TiO_3 irradiated by thermal neutron up to the fluence of $3.3 \times 10^{16} \text{ n cm}^{-2}$ with heating rate of 5 K min^{-1}

REFERENCES:

- [1] M. Oyaidzu et al., *J. Nucl. Mater.*, 375 (2008) 1
- [2] S. Suzuki et al., *Fusion Eng. Des.*, 85 (2010) 2331
- [3] M. Oyaidzu et al., *J. Nucl. Mater.*, 329 (2004) 1313
- [4] S. Fukada et al., *Journal of the Atomic Energy Society of Japan*, 51 (2009) 40

T. Nakamoto, M. Yoshida, T. Ogitsu, Y. Makida, Y. Kuno¹,
A. Sato¹, T. Itahashi¹, T. Hiasa¹, Q. Xu², K. Sato², Y.
Kuriyama², B. Qin², Y. Mori² and T. Yoshiie²

Cryogenics Section, J-PARC Center, KEK

¹Department of Physics, Osaka University

²Research Reactor Institute, Kyoto University

INTRODUCTION: Radiation resistant superconducting magnets will be crucial components for very high intensity muon experiments such as COMET at J-PARC and for high luminosity upgrade of the LHC accelerator at CERN. Neutron fluence on the superconducting magnets during the operational life is estimated to be around 10^{22} n/m². Since electrical resistivity of a stabilizer at low temperature, which is very sensitive to neutron irradiation, is one of the important parameters for the quench protection of the magnet system, increase of resistivity due to neutrons and its recovery behavior by a thermal cycle should be studied experimentally.

EXPERIMENTS: The irradiation test was carried out at a low temperature irradiation facility (LTL) at E-4 line of KUR. A sample with dimensions of 1 mm x 1 mm x 70 mm was cut from the aluminum stabilizer of the superconductor manufactured by Hitachi Cable. The aluminum stabilizer with a RRR of 500 is made from pure aluminum with Cu and Mg additives. A 4-wire method was used to measure the resistance. The temperature was determined using a CX-1050-SD CERNOX sensor placed just behind the sample. The sample with the thermometer was set at the end of a helium-gas cooling chamber.

RESULTS: After cooling down to 10 K, the reactor was turned on to a power of 1 MW. The resistance and the temperature changes during the irradiation are shown in Fig. 1. The temperature jumped from 10 K to 12 K at the beginning due to radiation from the reactor core. During irradiation, the temperature gradually increased at a rate of 0.07 K/hour, probably due to heating of the environment surrounding the sample chamber. The sample resistance ($R_{Meas.}$) was proportionally increased with the irradiation time fairly corresponding to the neutron fluence and finally reached to 5.7 $\mu\Omega$ at the end of the exposure. The resistance change due to the temperature rise ($R_{Temp.}$) is expected to be only 0.2 $\mu\Omega$ calculated using the temperature dependence measurement during cool-down without irradiation. Neutron fluence ($E_n > 0.5$ MeV) was determined to be 2.4×10^{20} n/m² by Ni foil activation method assuming

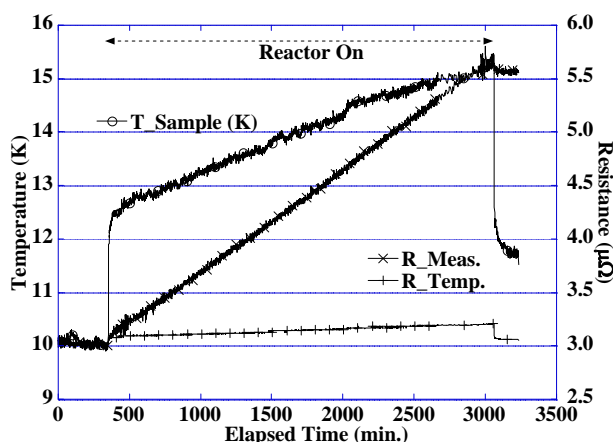


Fig. 1. Resistance and temperature of the aluminum sample during irradiation.

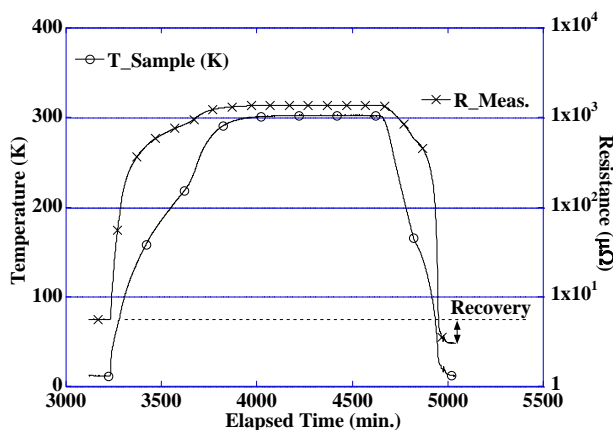


Fig. 2. Resistance and temperature of the aluminum sample during the subsequent thermal cycle after irradiation. Recovery of electrical resistance was verified.

Uranium fission spectrum. As a preliminary result, the resistance induced by the neutrons is determined to be 2.5 $\mu\Omega$: the resistivity was roughly doubled.

After the irradiation, the cryogenics was turned off and the sample was warmed up in the chamber for half a day. Then, the sample was cooled again to check the recovery of the resistance by the thermal cycle to ambient temperature. Figure 2 shows the trend of the sample resistance and temperature during the warm-up and cool-down periods. The resistance reached 3.0 $\mu\Omega$ after the cool-down. This value is fairly same as the one before the irradiation and is much lower than the one right after the irradiation. This means that the resistance increase of the sample due to the irradiation was fully recovered after the thermal cycle.

H. Ohashi, M. Haruta¹, T. Takei¹, T. Ishida¹, N. Kawakita¹, D. Kawamoto² and Y. Kobayashi³

Center for Research and Advancement in Higher Education, Kyushu University

¹Department of Applied Chemistry, Tokyo Metropolitan University

²Faculty of Sciences, Kyushu University

³Research Reactor Institute, Kyoto University

INTRODUCTION: Gold nanoparticles deposited on support often act as active sites of heterogeneous catalysts. Gold catalysts are usually prepared by deposition precipitation (DP) or co-precipitation (CP) method, which is the easiest and most commercial method in a lot of preparation methods. However, gold on activated carbon, which has high catalytic activities for mild oxidation of organic compounds have never been prepared by DP method.

Though sulfide deposition precipitation (SDP) method is a kind of new DP method, it is very unique method and different from DP on several points such as preparation pH.

The aim of this study is to prepare gold on activated carbon catalyst by SDP method and to investigate the chemical state of gold in this catalyst by ^{197}Au Mössbauer spectroscopy.

EXPERIMENTS: The catalysts were prepared by the SDP method already reported [1]. Au_2S_3 as a reference was prepared by usual depositing method, which used hydrochloric acid as precipitation reagent. The chemical state of gold in the solid samples was determined by ^{197}Au Mössbauer spectroscopy (home-made equipment). The ^{197}Pt isotope ($T_{1/2} = 18.3$ h), γ -ray source feeding the 77.3 keV Mössbauer transition of ^{197}Au , was prepared by neutron irradiation of isotopically enriched ^{196}Pt metal at the Kyoto University Reactor. The absorbers were particle specimens. The source and specimens were cooled with a helium refrigerator. The temperature of the specimens was in the range 8 – 15 K. The zero velocity point of the spectra was the peak point of pure bulk gold. The spectra for all the solid samples were fitted to a single Lorentzian function.

RESULTS: ^{197}Au Mössbauer spectra for Au_2S_3 , non-calcined Au/C and calcined Au/C catalysts are shown in Fig. 1. Though spectrum for non-calcined Au/C was not clear, it is similar to spectrum for Au_2S_3 , suggesting that Au_2S_3 was deposited on surface of activated carbon by SDP method. On the other hand, the chemical state of gold in calcined Au/C is only Au(0). By calcining the catalyst, Au_2S_3 on the surface was reduced to Au.

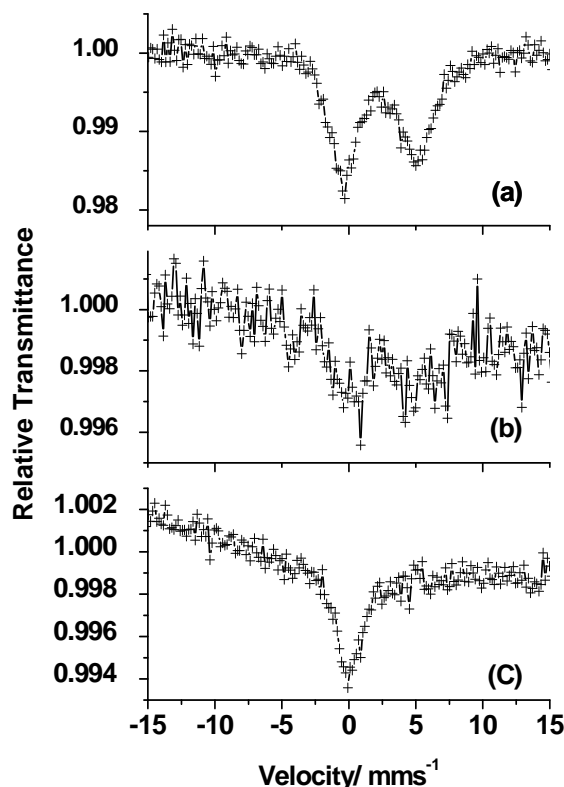


Fig. 1. ^{197}Au Mössbauer spectra for Au_2S_3 (a) as a reference and non-calcined (b) and calcined (c) Au/C prepared by SDP method.

REFERENCE:

[1] H. Ohashi, *et al.* Japanese Patent Disclosure (2009) 240951.

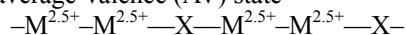
H. Iguchi, S. Takaishi, M. Yamashita, S. Kitao¹ and M. Seto¹

Graduate School of Science, Tohoku University

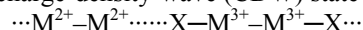
¹Research Reactor Institute, Kyoto University

INTRODUCTION: The charge-ordering (CO) state of quasi-one-dimensional (Q1D) halogen-bridged dinuclear metal complexes (MMX chains) have been extensively studied because they show multistability of various CO states and their response to external stimuli[1,2]. The CO states of the MMX chains can be classified into the following four states and are known to be strongly correlated to the position of the bridging halide ion.

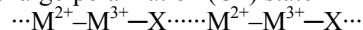
(a) average-valence (AV) state



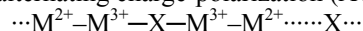
(b) charge-density-wave (CDW) state



(c) charge-polarization (CP) state



(d) alternating charge-polarization (ACP) state



Recently, the new CO state, ACP+CDW state[3], and reversible dehydration/rehydration properties[4] were discovered, though the details of the CO states have been unclear so far. Since ¹²⁹I Mössbauer spectroscopy is very sensitive to the charge of iodine atom and it has already been applied to general MMX chains [5,6], we measured the ¹²⁹I Mössbauer spectra of hydrated/dehydrated MMX chains to reveal the details of their CO states.

EXPERIMENTS: ¹²⁹I-enriched K₂(NC₃N)[Pt₂(pop)₄I]•4H₂O (**1•4H₂O**) (NC₃N = H₃NC₃H₆NH₃²⁺; pop = P₂O₅H₂²⁻) and K₂(cis-NC₄N)[Pt₂(pop)₄I]•4H₂O (**2•4H₂O**) (cis-NC₄N = cis-H₃NCH₂CH=CHCH₂NH₃²⁺) were synthesized from Na¹²⁹I aqueous solution in six steps. Dehydrated complex **1** and **2** were prepared by heating at 70 °C for a day under vacuum condition. The 27.7 keV γ-ray generated from ¹²⁹Te is used for ¹²⁹I Mössbauer spectrum. In this study, a ¹²⁹Te source was obtained by the neutron irradiation of enriched Zn¹²⁸Te in the nuclear reaction ¹²⁸Te[n,γ]¹²⁹Te at KURRI.

RESULTS: As shown in Fig. 1, ¹²⁹I Mössbauer spectrum of **1•4H₂O** consists of two chemically independent iodine sites. This result is consistent with the X-ray crystal structure analysis, indicating that **1•4H₂O** has Peierls-like distortion, which is one of the characteristic of ACP+CDW state. After the dehydration, two components of **1•4H₂O** changed to single components of **1**, indicating Peierls-like distortion vanished completely. This result supports the transition from ACP+CDW state to CDW state induced by dehydration.

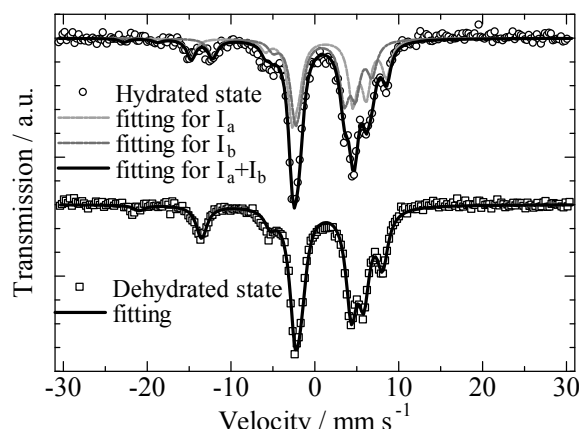


Fig. 1. ¹²⁹I Mössbauer spectra of **1•4H₂O** and **1** measured at 14 K.

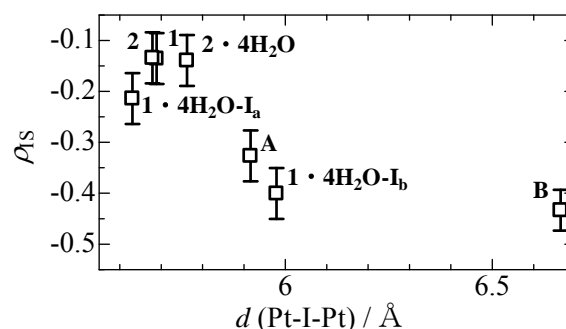


Fig. 2. $d(\text{Pt-I-Pt})$ - ρ_{IS} correlation diagram of MMX chains with pop ligand. Data A and B are reported value[6].

Figure 2 shows the relationship between Pt-I-Pt distance ($d(\text{Pt-I-Pt})$) and the charge on the ¹²⁹I calculated from isomer shift (ρ_{IS}). Contrast to dta-ligand system[9], ρ_{IS} was more positive in short $d(\text{Pt-I-Pt})$ for pop-ligand system, indicating that covalent bond interaction is dominant as $d(\text{Pt-I-Pt})$ becomes shorter.

REFERENCES:

- [1] H. Matsuzaki *et al.*, Phys. Rev. Lett., **90** (2003) 046401/1-4.
- [2] H. Mastuzaki *et al.*, Angew. Chem. Int. Ed., **44** (2005) 3240-3243.
- [3] H. Iguchi *et al.*, J. Am. Chem. Soc., **130** (2008) 17668–17669.
- [4] H. Iguchi *et al.*, Angew. Chem. Int. Ed., **49** (2010) 552-555.
- [5] H. Kitagawa *et al.*, J. Am. Chem. Soc., **121** (1999) 10068–10080.
- [6] A. Kobayashi *et al.*, Inorg. Chem., **48** (2009) 8044–8049.